Numerical and Experimental Analyses Examining Ozone and Limonene Distributions in Test Chamber with Various Turbulent Flow Fields

Kazuhide ITO [†]

Interdisciplinary Graduate School of Engineering Science, Kyushu University 6-1 Kasuga-koen, Kasuga, Fukuoka, 816-8580 Japan

Abstract

Indoor ozone has received attention because of its well-documented adverse effects on health. In addition to the inherently harmful effects of ozone, it can also initiate a series of reactions that generate potentially irritating oxidation products, including free radicals, aldehydes, organic acids and secondary organic aerosols (SOA). Especially, ozone reacts actively with terpene. The overarching goal of this work was to better understand ozone and terpene distributions within rooms. Towards this end, the paper has two parts. The first describes the development of a cylindrical test chamber that can be used to obtain the second order rate constant (k_b) for the bi-molecular chemical reaction of ozone and terpene in the air phase. The second consists of model room experiments coupled with Computational Fluid Dynamics (CFD) analysis of the experimental scenarios to obtain ozone and terpene distributions in various turbulent flow fields. The results of CFD predictions were in reasonable agreement with the experimental measurements.

Key words: Computational fluid dynamics, Ozone, Terpene, Model room experiment, Bi-molecular chemical reaction

Nomenclature

C_1 : ozone concentration [ppm]
C_2 : limonene concentration [ppm]
C_p : concentration of the hypothetical reaction products [ppm]
D_1 : molecular diffusion coefficient of ozone in the gas phase [m²/s]
D_2 : molecular diffusion coefficient of limonene in the gas phase [m²/s]
k_b : second order rate constant [1/ppm/s]
k_p : first order rate constant [1/s]
L_0 : representative length [m]
Re : Reynolds number ($= U_{in}L_0/\nu$) [-]
S : source term
U_{in} : air inlet velocity of chamber [m/s]
$\bar{U}_j$: ensemble-mean velocity [m/s]
u^* : friction velocity ($= \sqrt{\tau_w/\rho}$) [m/s]
$<v_T>$: Boltzmann velocity [m/s]

y^+ : wall unit ($= u^* y_1/\nu$) [-]
Δy_1 : distance to the center of the first computational cell [m]
γ : mass accommodation coefficient [-]
λ : mean molecular free path [m]
ν : kinematic viscosity [m²/sec]
ν_t : turbulent eddy viscosity [m²/sec]
ρ : air density [kg/m³]
σ_t : turbulent Schmidt number [-]
τ_w : wall shear stress

1. Introduction

Many studies have reported associations with ozone-initiated chemistry in indoor environments[1]. Ozone chemistry produces relatively short-lived products. Examples include primary and secondary ozonides, peroxyhemiacetals, α-hydroxy ketones, and peroxyacyl nitrates. Secondary organic aerosols are an important sub-group of stable products resulting from ozone-initiated chemistry. They are formed from low vapor-pressure oxidation products that par-

[†] Corresponding author. Tel.: +81 92 583 7628, Fax.: +81 92 583 7627
E-mail address: ito@kyudai.jp

tition between the gas phase and the surface of pre-existing aerosols or nucleate to form new aerosols[1-4]. The reaction of ozone with various terpenoids in indoor settings has been shown to contribute tens of $\mu g/m^3$ to the indoor concentration of sub-micron particles under appropriate conditions[5]. Sørensen and Weschler[6] and Ito[7,8] have used CFD simulations to examine the distribution of a hypothetical product resulting from the reaction of ozone with limonene. However, a major drawback to using numerical simulations is the lack of sufficient data on boundary conditions and also the lack of sufficient validation data of prediction accuracy.

The purpose of this study was to develop a numerical method based on CFD to predict ozone and terpene distributions and their chemical reactions in indoor environments. Towards this end, two different sets of experiments were conducted. First this study developed a reliable method, using a cylindrical test chamber, to examine ozone and terpene reactions in the air phase and estimate the corresponding second order rate constant (k_b) which represents the bi-molecular chemical reactions of ozone and terpene. The second study isolated the bi-molecular chemical reactions and measured the distribution of ozone and terpene within a two-dimensional model room. The results were subsequently used to validate a CFD model, corresponding to the experimental setup, which includes the chemical reactions of ozone and terpene in the air phase and the removal of ozone and terpene via surface deposition. In this study, d-limonene is targeted as reactive terpene.

2. Theory

2.1 Equation for ozone and terpene transport in indoor air

Assuming the concentration of ozone at a point in space to be C_1 [ppm], the transport of ozone is expressed by Equation (1):

$$\frac{\partial \bar{C}_1}{\partial t} + \frac{\partial \bar{U}_j \bar{C}_1}{\partial x_j} = \frac{\partial}{\partial x_j}\left(\left(D_1 + \frac{v_t}{\sigma_t}\right)\cdot\frac{\partial \bar{C}_1}{\partial x_j}\right) + S_1, \quad (1)$$

$$\frac{\partial \bar{C}_2}{\partial t} + \frac{\partial \bar{U}_j \bar{C}_2}{\partial x_j} = \frac{\partial}{\partial x_j}\left(\left(D_2 + \frac{v_t}{\sigma_t}\right)\cdot\frac{\partial \bar{C}_2}{\partial x_j}\right) + S_2 \quad (2)$$

Here, overbar (¯) denotes the ensemble-mean value. D_1 [m²/sec] is the molecular diffusion coefficient of ozone in the gas phase, $\bar{U}_j$ [m/sec] is the ensemble-mean velocity, v_t [m²/sec] is the turbulent eddy viscosity, and σ_t is the turbulent Schmidt number. S is the source term. The transport equation for limonene (C_2 [ppm]) is also the same (see Equation (2)).

2.2 Modeling the bi-molecular chemical reaction

The bi-molecular chemical reaction of ozone and limonene is expressed by Equation (3):

$$S_1 = S_2 = -k_b \cdot \bar{C}_1 \cdot \bar{C}_2 \quad (3)$$

Here, k_b is the second order rate constant [1/ppm/sec]. Equation (3) is incorporated within Equation (1) and (2) as the source term. From Equation (3), changes over time in the concentration of ozone "C_1" and limonene "C_2" due to the bi-molecular reaction are computed.

In addition, assuming the concentration of the hypothetical reaction products to be C_p [ppm], the amount of change over time is expressed by Equations (4) and (5). Here, k_p is the first order rate constant [1/sec] of the hypothetical reaction product C_p.

$$\frac{\partial \bar{C}_p}{\partial t} + \frac{\partial \bar{U}_j \bar{C}_p}{\partial x_j} = \frac{\partial}{\partial x_j}\left(\left(D_p + \frac{v_t}{\sigma_t}\right)\cdot\frac{\partial \bar{C}_p}{\partial x_j}\right) + S_p \quad (4)$$

$$S_p = k_p \cdot \bar{C}_p = k_b \cdot \bar{C}_1 \cdot \bar{C}_2 \quad (5)$$

2.3 Modeling the wall surface deposition flux

The surface deposition of the local concentration close to the surface, and from molecular theory, the flux at the surface is given by Cano-Ruiz et al.[9]:

$$J_d = -\gamma \cdot \frac{\langle v_T \rangle}{4} \cdot C_1\big|_{y=2\lambda/3} \quad (6)$$

Here, γ is the mass accommodation coefficient; $\langle v_T \rangle$ [m/s] is the Boltzmann velocity for ozone (or limonene); and λ [m] is the mean molecular free path of ozone (6.5×10^{-8} m). However, the grid scale (of the order of 10^{-8} m) is very small compared to the length scales necessary to resolve the flow field and concentration field within the CFD model. In this paper, to enable an increased length scale at the surface, the following flux model is adopted [6]. Here, Δy_1 is the distance to the center of the first computational cell ($\Delta y_1 < y^+ = 1$).

$$J = -\frac{\gamma \cdot \frac{\langle v_T \rangle}{4}}{1 + \gamma \cdot \frac{\langle v_T \rangle}{4} \cdot \frac{\Delta y_1}{D_1}} \cdot C_1 \Big|_{y=\Delta y_1} \qquad (7)$$

3. Methods

3.1 Overview of the cylindrical test chamber experiment

In order to estimate the second order rate constant of ozone and limonene, the cylindrical test chamber experiment is carried out. Figure 1 shows a perspective layout of the cylindrical test chamber. The cylindrical test chamber is a duct cavity and consists of three sections (55 mm (diameter) × 2,500 mm (length)) and these are connected using a U-bend. The inner boundaries for air passing through the chamber are made of electro-polished SUS 304 stainless steel. The air inlet velocity (U_{in}) was set at 1.0 m/s (Re=3850) and 0.25 m/s (Re=960). The inlet air and all the walls were maintained at isothermal conditions (293 ± 0.5 K). The supply air was passed through activated carbon and ULPA filters to keep the concentration of background contaminants low. In order to prevent photochemical reactions involving ozone, the experiments were carried out in a dark room. The points of measurement in the chamber are shown in Figure 1 (Positions (1)–(7)). The experimental cases are presented in Table 1. Ozone was analyzed using a UV Photometric Analyzer at a wavelength of 254 nm; its concentration range was 0 - 9.999 ppm, and its precision was 0.001 ppm. The sampling flow rate of the UV Photometric Analyzer was 1.5 L/min and the ozone concentration was calculated as a time-averaged concentration over ten minutes. The adsorption sampling using Carbtrap349 (Gestel) and GC/MS (Agilent Tech.) were used to measure the d-limonene. A Wide-range Particle Spectrometer (WPS, MSP) was used to monitor background particles (10 nm -10 μm diameter.).

These experiments focused on the heterogeneous reactions between ozone (or limonene) and the inner surface of the chamber (Cases 1-1(c), 1-2(c), 2-1(c) and 2-2(c)) and homogeneous reactions between ozone and limonene in the air phase (Cases 1-3(c) and 2-3(c)).
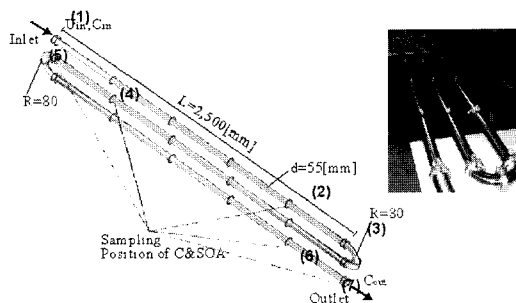

Fig. 1. Schematic of cylindrical test chamber.

Table 1. Cases analyzed in the cylindrical test chamber experiment.

Case	Supply Inlet Vel.	Ozone	d-Limonene
Case 1-1(c)		1.00 [ppm]	-
Case 1-2(c)	U_{in}=1.00 [m/s]	-	19.5 [μg/s]
Case 1-3(c)		1.00 [ppm]	19.5 [μg/s]
Case 2-1(c)		5.00 [ppm]	-
Case 2-2(c)	U_{in}=0.25 [m/s]	-	8.1 [μg/s]
Case 2-3(c)		5.00 [ppm]	8.1 [μg/s]

3.2 Overview of the model room experiment

In order to measure the validation data of numerical prediction, the model room experiment is carried out. The model room is shown in Figure 2a; it is a box measuring 1.5 m (x) × 0.3 m (y) × 1.0 m (z) in which a two-dimensional mean flow field is developed. It is equipped with 0.02 m wide inlet and outlet slots. The supply inlet slot is positioned along the ceiling, and the exhaust outlet slot is set along the ceiling on the opposite sidewall. The four boundaries for air flowing through the room – ceiling, floor, right, and left walls – were made of SUS 304 stainless steel and the ends were glass. These experiments assumed that ozone entered the room from outdoors with the ventilation air and measured the resulting distribution of ozone concentrations in the model room. Limonene was emitted within the room (see Figure 2a). The air inlet velocity was controlled at either 3.0 m/s (144 air changes/hour; the turbulent intensity of the supply inlet flow was 0.015, Re=4200) or 2.0 m/s (96 air changes /hour, Re=2800). The inlet air and walls were controlled to maintain isothermal conditions (293 ± 1.0 K). The relative humidity of the supplied air was maintained at 30 ± 5%. Contaminants in the supply air (i.e., VOCs and suspended particulate matter) were removed by an active carbon filter and a ULPA

filter. In order to prevent photochemical reactions, the model room experiments were carried out in the dark. The central section in the Y direction is taken as the measurement plane (x - z plane in Figure 2a). Points of measurement in the model room are shown in Figure 2c.

We conducted detailed measurements of the flow fields in the model room using Laser Doppler Velocimetry (LDV); as a consequence numerous statistical data related to the turbulent flow as well as the

(a) Schematic of model room

(b) Photo of external appearance

(c) Sampling locations of ozone and limonene

Fig. 2. Experimental setup of model room.

average air velocity are available. Details of the modeling experiment for flow fields were reported in Ito et al.[10]. In the model room, a large circulating flow was formed along the wall surface in the room, and a secondary vortex against the major flow was observed in the floor corner.

The experimental cases are shown in Table 2. In all the experimental cases, the measurements were focused on the convection and diffusion of ozone contained in the supply air and its deposition on the wall surfaces and bi-molecular chemical reaction with limonene. The ozone was produced by an ozone generator and the ozone concentration in the supply air, C_{in}, was maintained at a constant 0.30 ppm. At the air supply slot position, the ozone concentration was measured in the y and z directions to confirm that uniformity was maintained. The ozone concentration was always monitored in the center of the air supply slot and fluctuation with time was also checked. It was confirmed that C_{in} was within about a 2% range of the target concentration over the period of the experiments. The limonene was produced by line source on the floor level. In these experiments measurements of ozone and limonene concentrations at the different sampling points were conducted for approximately one hour after introducing ozone/ limonene to the room in order to confirm that these concentrations had reached a steady state.

The sampling and analytical methods of ozone and limonene were the same as for the cylindrical test chamber experiment. Prior to measuring ozone / limonene concentrations, the model room was cleaned with neutral detergent and pure water. In each case the ozone concentration was measured at 11 points, including the supply inlet and exhaust outlet positions as shown in Figure 2c.
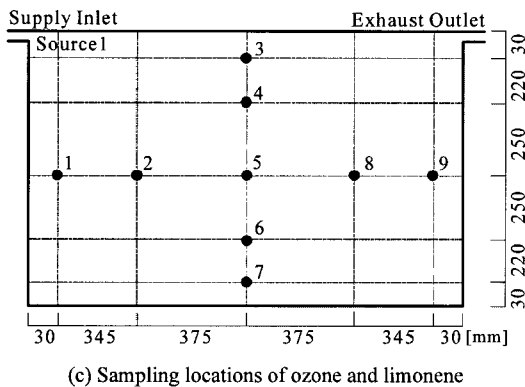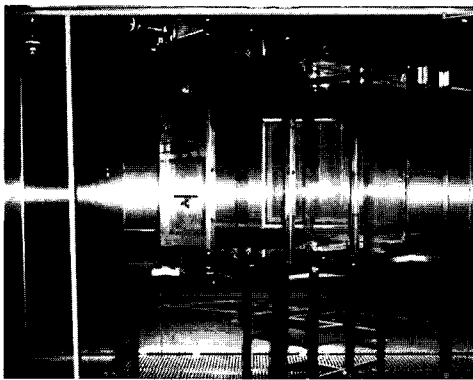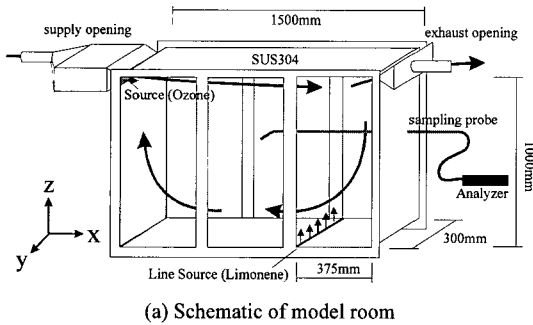
Table 2. Cases analyzed in the model room experiment.

Case	Supply Inlet Vel.	Ozone	d-Limonene
Case 1-1(e)		0.30 [ppm]	-
Case 1-2(e)	U_{in}=2.0 [m/s]	-	15.6 [μg/s]
Case 1-3(e)		0.30 [ppm]	15.6 [μg/s]
Case 2-1(e)		0.30 [ppm]	-
Case 2-2(e)	U_{in}=3.0 [m/s]	-	15.6 [μg/s]
Case 2-3(e)		0.30 [ppm]	15.6 [μg/s]

3.3 Overview of the numerical analysis for the model room

Flow fields were analyzed using the low Reynolds number type k-ε model[11]. The QUICK scheme is used for the convection term, and a SIMPLE algorithm is used. To analyze the flow field in the boundary layer, the center of the computational cells closest to the wall surface should be at a non-dimensional distance (Wall Unit) of $y^+<1$, where $y+ = u * y_1/v$, and y_1 is the distance normal to the wall surface, v is the kinematic viscosity, and $u* = \sqrt{\tau_w/\rho}$ is the friction velocity. Here, ρ is the air density and τ_u is the wall shear stress. The number of meshes was set to 220 $(x) \times$ 110 (z), and an unequal interval mesh is used for this analysis. In this analysis, the height of the cells closest to the ceiling wall surface is 6.0×10^{-6} m. The analysis was carried out in two dimensions for the central plane (the x-z plane in Figure 2a) of the model room in the y direction. When the air supply slot width is the representative length (L_0 = 0.02 m), the analytical space is a two-dimensional room measuring 75 L_0 $(x) \times$ 50L_0 (z) (equal to 1.5 m ×1.0 m). The air inlet velocity were set to U_{in} = 2.0 and 3.0 m/s, which are the same inlet velocities that were used in the experiments. The turbulence intensity was set to 1.5% based on the experimental results. Numerical cases in the model room are shown in Table 3. Mass accommodation coefficient against SUS 304 are defined as 3.4×10^{-6} [-] for ozone and 2.1×10^{-5} [-] for limonene corresponding to previous reported values[12].

4. Results

4.1 Cylindrical test chamber experiment

The background concentration of the sum of the airborne organic compounds, i.e. TVOC, was confirmed to be below 30 μg/m³, while the particulate matter in the supply air was below the detection limit of the Wide-range Particle Spectrometer. Hence, gas phase reactions of ozone (except for reactions with limonene), as well as reactions on particle surfaces, were negligible in the cylindrical test chamber experiment.

Table 4 shows the average concentration of ozone and limonene at the sampling points (see Figure 1). In Case 1-1(c) and Case 2-1(c), in which only ozone was introduced to the chamber, the measured concentration decays were caused by wall surface deposition on the inner SUS304 surfaces. Correspondingly, in Case 1-2(c) and Case 2-2(c), in which only limonene was introduced to the chamber, the measured concentration decays were also caused by wall surface deposition. The concentration decrease while air passed from inlet (1) at outlet (7) became about 10% for Case 1-1(c), and 10 -15% for Case 1-2(c). In Case 1-3(c), in which ozone and limonene were supplied at the same time from the supply inlet, the decrease in the concentrations of ozone and limonene grew rapidly, and the concentration decrease from inlet (1) to outlet (7) became about 60% for ozone and 40% for limonene. [NOTE1] In Case 1-3(c), secondary organic aerosols (SOA) formation that originated in the chemical reactions of ozone and limonene was observed.

Using the data for the averaged concentration of ozone and limonene at each sampling point in the chamber, the second order rate constant (k_b) for the bi-molecular chemical reaction of ozone and limonene in the air phase was estimated according to Equation (8). The concentration changes over time were calculated by using the pre-estimated data on the age of the air in Table 4.

$$\frac{\partial C_1}{\partial t} = \frac{\partial C_2}{\partial t} = -k_b \cdot C_1 \cdot C_2 \qquad (8)$$

Table 3. Information related to numerical analysis.

Turbulence Model	Low Re Type k-ε model (MKC model, 2-Dimensional Cal.)		
Mesh	220 $(x) \times$ 110 (z)		
Scheme	Convection Term: QUICK		
Inflow Boundary	U_{in} = 3.0 [m/s] and 2.0 [m/s] k_{in}=3/2× $(U_{in}×0.015)^2$, ε_{in}=C_μ×$k_{in}^{3/2}$/l_{in}, C_μ=0.09, l_{in}=L_0 (Slot Width: 0.02) ×1/7		
Outflow Boundary	U_{out}= free slip, k_{out}= free slip, ε_{out}= free slip		
Wall Treatment	Velocity; No-slip, $k\|_{wall}$; no slip, $\varepsilon\|_{wall}$ = $2v(\partial\sqrt{k}/\partial y)^2$ Limonene: $<v_T>$ = 213.4 [m/s], γ = $2.1×10^{-5}$ [-] Ozone: $<v_T>$ = 360.0 [m/s], γ = $3.4 ×10^{-6}$ [-]		

Table 4. For each of the experimental cases, ozone, limonene and SOA concentrations at each sampling point (cylindrical test chamber experiment).

Sampling Point	Inlet (1)	(2)	(3)	(4)	(5)	(6)	Outlet (7)
Case 1-1(c) (Ozone)[ppm]	1.00	0.96	0.95	0.98	0.95	0.97	0.88
Case 1-2(c) (limonene)[ppm]	(1.75)	1.45	1.66	1.68	1.74	1.46	1.57
Case 1-3(c) (Ozone) [ppm]	1.00	0.50	0.49	0.44	0.42	0.39	0.39
Case 1-3(c) (limonene)[ppm]	(1.75)	1.22	1.46	1.41	1.53	1.41	1.10
Case 1-3(c) (SOA)[mg/m³]	-	1.92	2.07	5.14	5.74	7.32	7.50
Age of Air [sec]	0.00	2.06	2.51	4.78	5.23	7.50	7.99
k_b [1/ppm/sec] (Ozone)	-	2.4×10^{-1}	1.9×10^{-1}	1.1×10^{-1}	1.0×10^{-1}	7.8×10^{-2}	9.2×10^{-2}
(Lim)	-	3.6×10^{-1}	1.3×10^{-1}	7.5×10^{-2}	3.8×10^{-2}	7.7×10^{-2}	1.1×10^{-1}
Y [-] (Ozone)	-	3.47	3.61	8.65	8.89	11.16	10.02
(Lim)	-	2.26	5.31	12.23	24.35	11.34	8.82
Case 2-1(c) (Ozone)[ppm]	5.00	4.82	4.91	4.79	4.83	4.81	4.84
Case 2-2(c) (limonene)[ppm]	(2.92)	2.08	2.23	2.03	2.26	2.07	2.19
Case 2-3(c) (Ozone)[ppm]	5.00	2.91	-	-	-	-	-
Case 2-3(c) (limonene)[ppm]	(2.92)	1.74	2.10	1.80	2.20	1.54	2.04
Case 2-3(c) (SOA [mg/m³]	-	70.30	75.53	103.26	107.29	110.03	113.08
Age of Air [sec]	0.00	8.24	10.04	19.12	20.92	30.00	31.96
k_b [1/ppm/sec] (Ozone)	-	3.0×10^{-2}	-	-	-	-	-
(Lim)	-	1.1×10^{-2}	2.7×10^{-3}	3.7×10^{-3}	7.8×10^{-4}	3.2×10^{-3}	1.1×10^{-3}
Y [-] (Ozone)	-	30.2	-	-	-	-	-
(Lim)	-	80.7	216.7	119.9	498.4	101.3	250.7

In Case 1(c), k_b estimated from the decrease in concentration of ozone ranged from 1.9×10^{-1} from 7.8×10^{-2} [1/ppm/sec], and was 1.3×10^{-1} [1/ppm/sec] on average. k_b estimated from the decrease in concentration of limonene ranged from 3.6×10^{-1} to 7.5×10^{-2} [1/ppm/sec], and was 1.3×10^{-1} [1/ppm/sec] on average. This was reasonably consistent with the k_b estimated from the ozone data. In Case 2(c), k_b estimated from experimental data for ozone was 3.0×10^{-2} [1/ppm/sec] and k_b estimated from the experimental data on limonene ranged from 1.1×10^{-2} to 7.8×10^{-4} [1/ppm/sec], and was 3.8×10^{-3} [1/ppm/sec] on average. In this estimation, k_b is time dependent.

Atkinson et al.[13] report the measurements results of k_b for ozone and limonene to be 2.1×10^{-16} [cm³molecules⁻¹sec⁻¹] = 5.1×10^{-3} [1/ppm/sec, 296 K] and the order of this value is close to the estimated result in Case 2(c).

Using the data for the average concentration of SOA at each sampling point, the fractional aerosol yield (Y) was estimated from Equation (9). The estimated results are shown in Table 4.

$$\frac{\partial C_{SOA}}{\partial t} = Y \cdot \frac{\partial C_p}{\partial t} = Y \cdot \left(k_b \cdot C_1 \cdot C_2 \right), \quad Y = \frac{\Delta C_{SOA}}{\Delta C_p} \quad (9)$$

4.2 Model room experiment

The measured ozone and limonene concentrations at the various sampling points within the model room are shown in Figure 3; each measurement was made at least three times to ensure reproducibility. Ozone deposition on the glass surfaces in the model room was negligible. In addition, the level of TVOC in the supply air was quite low. Therefore, the dominant cause for the reduction in ozone concentration in the model room was deposition onto the surfaces of the SUS304 installed on the wall surfaces in Case 2-1(e) and Case 1-1(e). In all experimental cases, non-uniform concentration distributions were generated in the model room.

In terms of the ozone concentrations at the exhaust outlet position, the decreases in ozone concentration were about 4% in Case 2-1(e) and 9% in Case 2-3(e). This difference in the decrease in the ozone concentration originates in the bi-molecular chemical reactions of ozone and limonene. In Case 2, similar tendencies were observed.
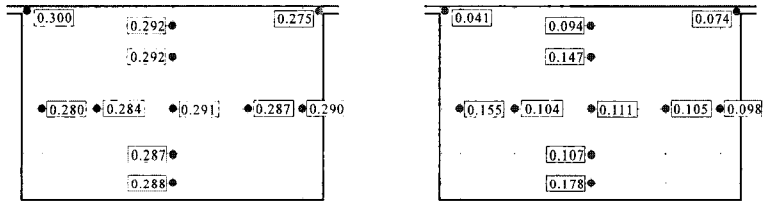
4.3 Numerical analysis for the model room

Figure 4b shows the analysis results for the flow
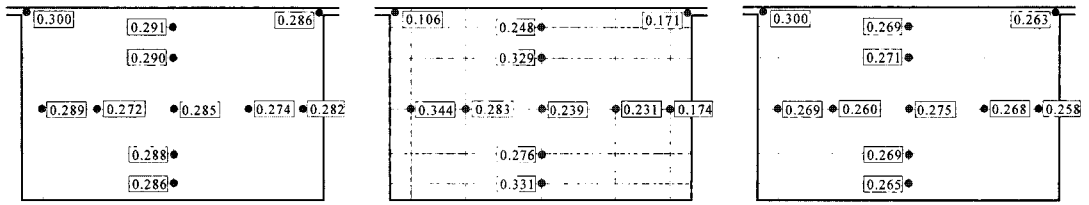
(1) Case 1-1 (e), (U_{in}=2.0 m/s, Ozone)   (2) Case 1-2 (e), (U_{in}=2.0 m/s, Lim)   (3) Case 1-3 (e), (U_{in}=2.0 m/s, Ozone, react)
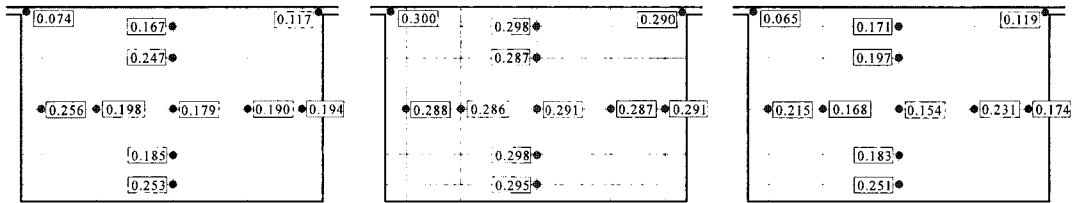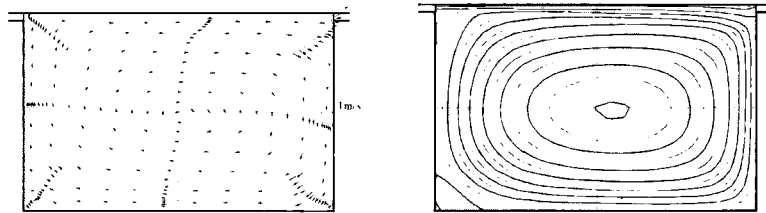
(4) Case 1-3 (e), (U_{in}=2.0 m/s, Lim, react)   (5) Case 2-1 (e), (U_{in}=3.0 m/s, Ozone)   (6) Case 2-2 (e), (U_{in}=3.0 m/s, Lim)
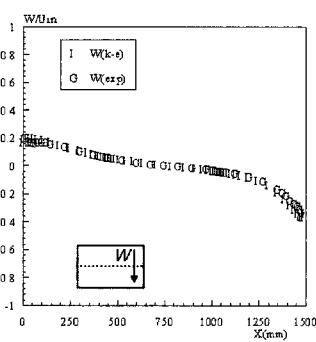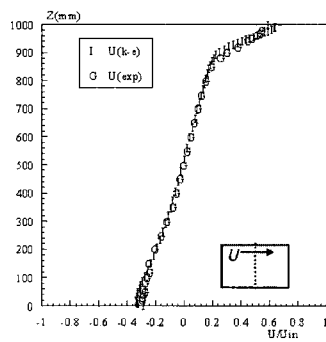
(7) Case 2-3 (e), (U_{in}=3.0 m/s, Ozone, react)   (8) Case 2-3 (e), (U_{in}=3.0 m/s, Lim, react) [ppm]

Fig. 3. Measured concentrations of ozone and limonene [ppm] in the model room.

(a) Flow field measured by LDV   (b) Stream Line Predicted by CFD

(c) U/U_{in} (x=750mm Line)   (d) W/U_{in} (z=500mm Line)

Fig. 4. Flow field as determined by experiment and theory.

field using the Low-Re Type k-ε model, and Figures 4c and 4d show comparisons between the experimental results and the theoretical results. These comparisons confirm that the results for the flow field based on CFD analysis accurately reproduce the flow field measured inside the model room.

Figure 5 shows the results of the numerical analyses for the ozone and limonene concentration distributions in two dimensional model room. In all of the cases, ozone would have been uniformly distributed inside the room if there were no deposition flux, expressed by Equation (7), or bi-molecular chemical reaction with limonene. In this analysis, the k_b value estimated by Atkinson et al.[13] was adopted because the order of the value was close to the estimated result in cylindrical test chamber experiment. The mass accommodation coefficient γ of ozone and limonene onto the SUS 304 wall surfaces, which was estimated
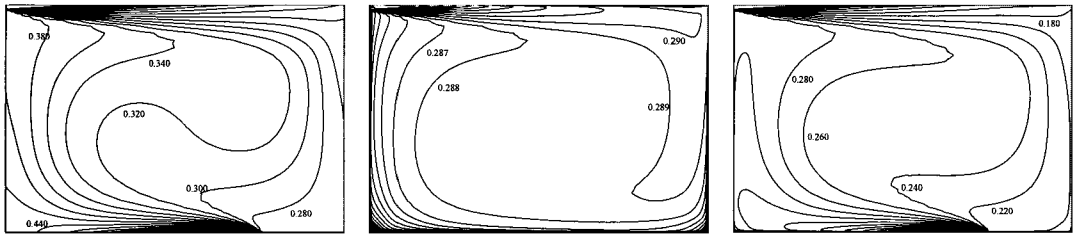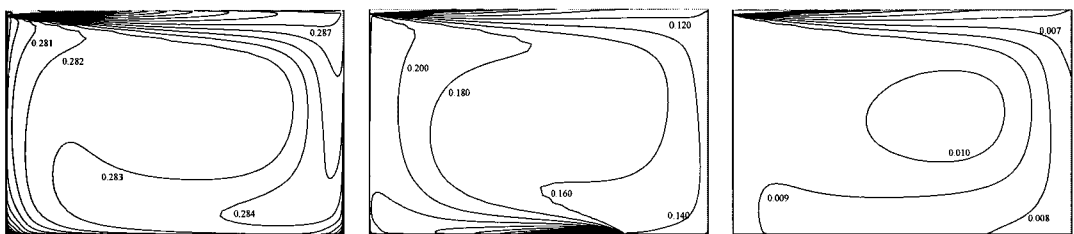

(1) Case 1-b (a), (U_{in}=2.0 m/s, Lim, no-dep) (2) Case 1-1 (a), (U_{in}=2.0 m/s, Ozone, dep) (3) Case 1-2 (a), (U_{in}=2.0 m/s, Lim, dep)
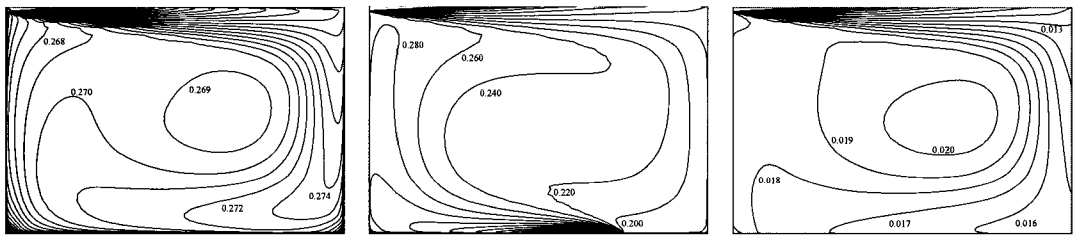
(4) Case 1-3 (a), (U_{in}=2.0 m/s, Ozone, react) (5) Case 1-3 (a), (U_{in}=2.0 m/s, Lim, react)   (6) Case 1-3 (a), (U_{in}=2.0 m/s, Prods, react)
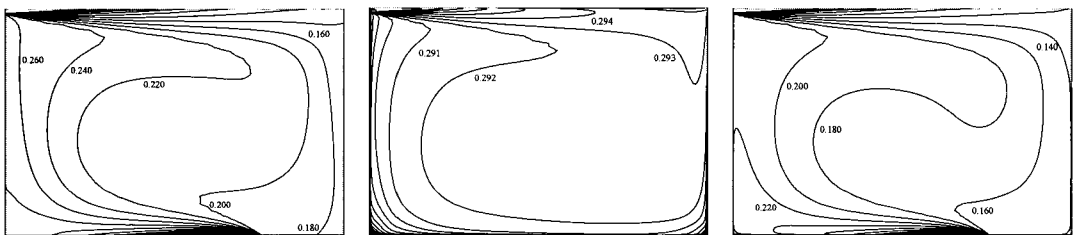
(7) Case 2-b (a), (U_{in}=3.0 m/s, Lim, no-dep) (8) Case 2-1 (a), (U_{in}=3.0 m/s, Ozone, dep) (9) Case 2-2 (a), (U_{in}=3.0 m/s, Lim, dep)

(10) Case 2-3 (a), (U_{in}=3.0 m/s, Ozone, react)   (11) Case 2-3 (a), (U_{in}=3.0 m/s, Lim, react) (12) Case 2-3 (a), (U_{in}=3.0 m/s, Prods, react)

Fig. 5. CFD-determined ozone and limonene concentration (ppm) distributions in the model room.
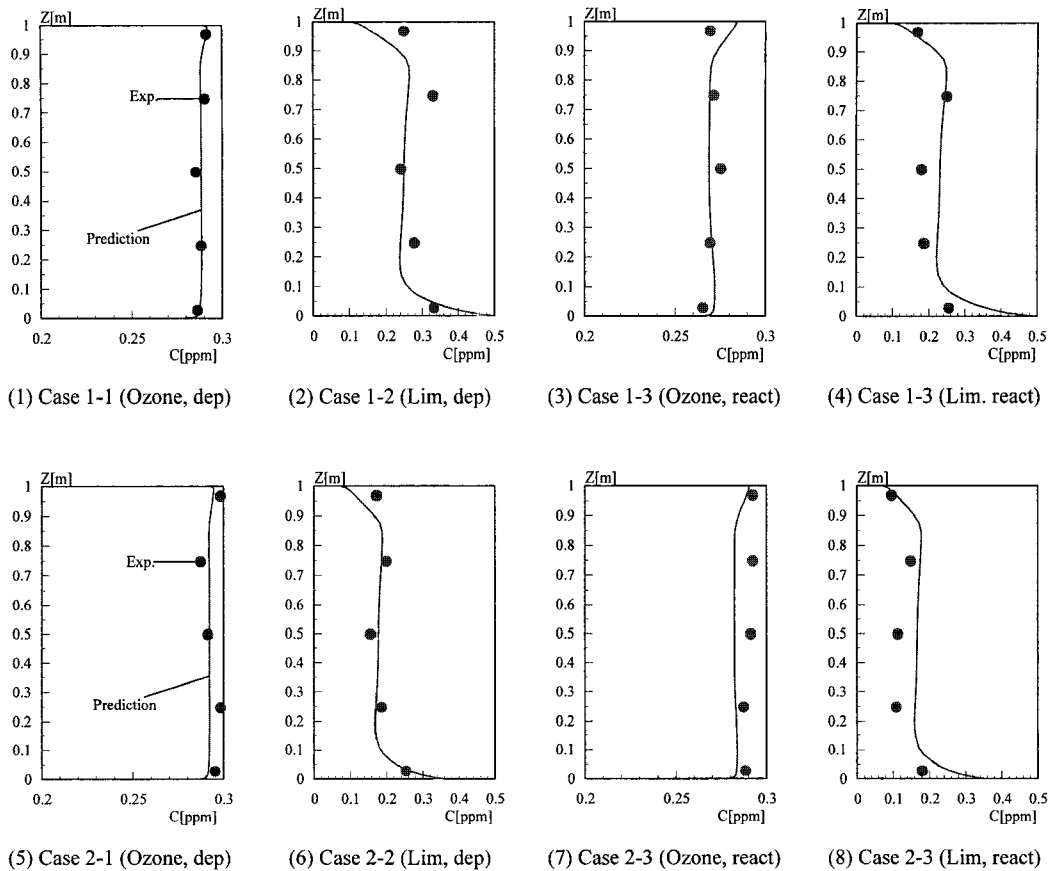
(1) Case 1-1 (Ozone, dep)   (2) Case 1-2 (Lim, dep)   (3) Case 1-3 (Ozone, react)   (4) Case 1-3 (Lim. react)

(5) Case 2-1 (Ozone, dep)   (6) Case 2-2 (Lim, dep)   (7) Case 2-3 (Ozone, react)   (8) Case 2-3 (Lim, react)

Fig. 6. Measured (dots) and predicted (lines) ozone and limonene concentrations. (x=750 mm, z=0 to 1000 mm) for different cases in the model room.

using the flat plate test chamber in the experiment conducted by Ito et al.[12], were used in this analysis.

Based on the results from the numerical analysis, Table 5 shows the average ozone concentration in the room as well as at a point in the exhaust outlet; it also presents the relative amount of ozone and limonene removed by ventilation, by deposition onto the wall surfaces and by chemical reaction. Case 1-b(a) and Case 2-b(a) in which only limonene was generated in model room and there were no deposition flux were additional and reference numerical cases of Case 1-2(a) and Case 2-2(a). Under the outlined analysis conditions, in Case 2-1(a), in which an SUS 304 wall surface was installed, the relative amount removed by ventilation was 97.7%, while the amount removed by deposition onto the SUS 304 wall was 2.3%. In Case 2-2(a), in which limonene was emitted into the model room, the relative amount removed by ventilation was 81.8%, while the amount removed by deposition onto the SUS 304 wall was 18.2%.

In Case 2-3(a), in which ozone and limonene were supplied at the same time, the relative amount removed by chemical reaction was 2.0%. Under these analytical conditions, the amounts of chemical reaction of ozone and limonene were relatively small because of the high supply inlet velocity and short nominal time constant of the model room.

In Case 1-3(a), in which supply inlet velocity was set relatively low compared with Case 2-3(a), concentration reduction by chemical reaction increased because of longer nominal time constant.

We confirmed that the flow field analysis based on CFD matches the experimental measurements reasonably well. Therefore, if there are estimation errors in the numerical analysis, the difference from the experimental results can be attributed to that part of the numerical model that accounts for ozone and limonene loss and the predicted accuracy of the model parameters (k_b and γ).

Table 5. For each of the simulated cases, ozone and limonene concentrations at the exhaust outlet, average concentration in the room and removal ratio.

Anal. Case	Inlet Vel.	Ozone	Limonene	C_{ave} [ppm]	C_{ext} [ppm]	Removal Ratio [%]	
Case 1-b(a)	U_{in}=2.0 [m/s]	-	q_L=15.64 [μg/s] γ = 0	- [O] 0.326 [L]	- [O] 0.231 [L]	Ventilation Wall Dep. Chem. React	: 100.0 [L] : 100.0 [L] : 100.0 [L]
Case 1-1(a)		C_{in}=0.30 [ppm] γ=3.4×10^{-6} [-]	-	0.288 [O] - [L]	0.289 [O] - [L]	Ventilation Wall Dep. Chem. React	: 196.3 [O] : 103.7 [O] : 100.0 [O]
Case 1-2(a)		-	q_L=15.64 [μg/s] γ=2.1×10^{-5} [-]	- [O] 0.254 [L]	- [O] 0.176 [L]	Ventilation Wall Dep. Chem. React	: 176.2 [L] : 123.8 [L] : 100.0 [L]
Case 1-3(a)		C_{in}=0.30 [ppm] γ=3.4×10^{-6} [-] k_b=5.1×10^{-3} [1/ppm/sec]	q_L=15.64 [μg/s] γ=2.1×10^{-5} [-]	0.271 [O] 0.238 [L] 0.018 [P]	0.278 [O] 0.165 [L] 0.012 [P]	Ventilation Wall Dep. Chem. React	: 192.6 [O] : 171.4 [L] : 103.4 [O] : 124.6 [L] : 104.0 [O] : 104.0 [L]
Case 2-b(a)	U_{in}=3.0 [m/s]		q_L=15.64 [μg/s] γ = 0	- [O] 0.217 [L]	- [O] 0.154 [L]	Ventilation Wall Dep. Chem. React	: 100.0 [L] : 100.0 [L] : 100.0 [L]
Case 2-1(a)		C_{in}=0.30 [ppm] γ=3.4×10^{-6} [-]	-	0.292 [O] - [L]	0.293 [O] - [L]	Ventilation Wall Dep. Chem. React	: 197.7 [O] : 102.3 [O] : 100.0 [O]
Case 2-2(a)		-	q_L=15.64 [μg/s] γ=2.1×10^{-5} [-]	- [O] 0.180 [L]	- [O] 0.126 [L]	Ventilation Wall Dep. Chem. React	: 181.8 [L] : 118.2 [L] : 100.0 [L]
Case 2-3(a)		C_{in}=0.30 [ppm] γ=3.4×10^{-6} [-] k_b=5.1×10^{-3} [1/ppm/sec]	q_L=15.64 [μg/s] γ=2.1×10^{-5} [-]	0.283 [O] 0.172 [L] 0.009 [P]	0.287 [O] 0.120 [L] 0.006 [P]	Ventilation Wall Dep. Chem. React	: 195.7 [O] : 177.9 [L] : 102.3 [O] : 120.1 [L] : 102.0 [O] : 102.0 [L]

[O] : Ozone, [L] : Limonene, [P] : Hypothetical Products, [Wall Dep.] : Wall Surface Deposition, [Chem. React] : Chemical Reaction

5. Conclusions

A numerical method based on CFD to predict ozone and limonene distributions and their chemical reactions in indoor environments was proposed in this study. In order to estimate the model parameters and to provide the validation data of numerical predictions, two different sets of experiments were conducted.

The findings obtained from the cylindrical test chamber study can be summarized as follows:

(1) This work has produced a reliable method which permits estimations of the second order rate constant (k_b) for bi-molecular chemical reactions in the gas phase based on the concentrations measured along the stream line in the chamber.

(2) The k_b values for ozone and limonene reactions were estimated to be between 1.3×10^{-1} and 7.8×10^{-4} [1/ppm/sec]. The value was 3.8×10^{-3} [1/ppm/sec] on the average and was confirmed to

be almost identical to the values of k_b reported by Atkinson.

The findings obtained from the model room experiments and companion CFD studies can be summarized as follows:

(3) The reduction in the ozone and limonene concentration and these concentration distributions in the model room were measured.

(4) A numerical analysis was conducted that incorporated the deposition flux model for a wall surface and the bi-molecular chemical reaction model based on k_b. Measured results from the model room experiments were used to verify the accuracy of the numerical analysis. Although the modeled results tended to overestimate the concentration change in the vicinity of the wall surface, predicted concentrations of ozone and limonene were reasonably consistent with the experimental results in the center part of the model room.

(5) CFD prediction coupled with chemical reaction model was confirmed to become a powerful tool to predict both the distributions of reactive chemical pollutants in indoor environment and occupant health.

Acknowlegdement

Note

1. In Table 4, the concentrations of ozone and limonene tended to fluctuate according to the sampling point for some cases. This phenomenon was mainly caused by non-uniform concentration distribution at cross-sectional surface of each sampling point. According to CFD analysis, the concentration gradient of about 10% or less was confirmed around the sampling point. The experimental results in this paper came to have the uncertainty at this level.

References

[1] Weschler CJ (2000a). Ozone in Indoor Environments: Concentration and Chemistry. International Journal of Indoor Air Environment and Health, Indoor Air *10* (4), pp. 269-288.

[2] Weschler CJ, and Shields HC (2000b). The Influence of Ventilation on Reactions Among Indoor Pollutants, Modeling and Experimental Observation. Indoor Air *10* (2), pp. 92-100.

[3] Weschler CJ (2004). Chemical Reactions Among Indoor Pollutants: What We've Learned in the New Millennium. Indoor Air *14* (Suppl 7), pp. 184-194.

[4] Wolkoff P, Clausen PA, Wilkins CK, Hougaard KS, and Nielsen G.D (1999). Formation of Strong Airway Irritants in a Model Mixture of (+) –α-pinene/Ozone. Atmospheric Environment, *33*, pp. 693-698.

[5] Weschler CJ, (2006) Ozone's Impact on Public health: Contributions from Indoor Exposures to Ozone and Products of Ozone- Initiated Chemistry, Environmental Health Perspectives, Colume 114, Number *10*, pp1489-1496

[6] Sørensen DN and Weschler CJ (2002). Modeling Gas Phase Reactions in Indoor Environments Using Computational Fluid Dynamics. Atmospheric Environment, *36* (1): 9-18

[7] Ito K., (2007a) Experimental and CFD Analyses Examining Ozone Distribution in 2D Model Room with Laminar and Turbulent Flow Field : Journal of Asian Architecture & Building Engineering, *JAABE*, vol. 6, no.2, pp 387-394

[8] Ito K., (2007b) Experimental and CFD Analyses Examining Ozone and Terpene Distributions in Model Rooms with Laminar and Turbulent Flow Fields: IAQVEC 2007, pp302

[9] Cano-Ruiz JA, Kong D, Balas RB, Nazaroff WW (1993). Removal of Reactive Gases at Indoor Surfaces: Combining Mass Transport and Surface Kinetics. Atmospheric Environment *27*A (13), 2039-2050

[10] Ito K, Kato S, and Murakami S (2000). Model Experiment of Flow and Temperature Field in Room for Validating Numerical Simulation Analysis of Newly Proposed Ventilation Effectiveness. J. Archit. Plann. Environ. Eng., Architectural Institute of Japan, No. 534, 49-56

[11] Murakami S, Kato S, and Chikamoto T (1996). New Low Reynolds-number k-ε Model Including Damping Effect Due to Buoyancy in a Stratified Flow Field. Int. J. Heat Mass Transfer, *39*, 3483-3496.

[12] Ito K, Sørensen DN, Weschler CJ. (2005) Measurements of Mass Accommodation Coefficients Using a Flat-Plate Test Chamber : Indoor Air 2005, China, 2335-2339

[13] Atkinson R, Hasegawa D, and Aschmann S.M (1990) Rate constants for the gas-phase reactions of O3 with a series of monoterpenes and related compounds at 296 K, International Journal of Chemical Kinetics, *22*, 871